Journal of the Taiwan Institute of Chemical Engineers 68 (2016) 80–89

Contents lists available at ScienceDirect

Journal of the Taiwan Institute of Chemical Engineers

journal homepage: www.elsevier.com/locate/jtice

Batch and column studies for the adsorption of chromium(VI) on low-cost Hibiscus Cannabinus kenaf, a green adsorbent

Mohammad Omidvar Borna[a], Meghdad Pirsaheb[b], Mehdi Vosoughi Niri[c,d], Reza Khosravi Mashizie[e], Babak Kakavandi[c,d], Mohammad Reza Zare[f], Anvar Asadi[b,*]

[a] Department of Environmental Health, Gharb Petroleum Industry Health Organization, Kermanshah, Iran
[b] Department of Environmental Health Engineering, Faculty of Public Health, Kermanshah University of Medical Sciences, Kermanshah, Iran
[c] Department of Environmental Health Engineering, School of Health, Ahvaz Jundishapur University of Medical Sciences, Ahvaz, Iran
[d] Student Research Committee, Ahvaz Jundishapur University of Medical Sciences, Ahvaz, Iran
[e] Bardsir Health Center, Kerman University of Medical Sciences, Kerman, Iran
[f] Department of public health, Evaz school of health, Larestan school of medical sciences, Larestan, Iran

ARTICLE INFO

Article history:
Received 7 May 2016
Revised 8 September 2016
Accepted 20 September 2016
Available online 4 October 2016

Keywords:
Hibiscus Cannabinus kenaf
Hexavalent chromium
Batch adsorption
Fixed-bed column
Regeneration efficiency

ABSTRACT

Adsorption is one of the excellent ways for heavy metal removal from aqueous solution because of advantages like the low cost, availability, profitability, ease of operation and efficiency. In this study, adsorption potential of a low cost adsorbent Hibiscus Cannabinus kenaf was investigated for Cr(VI) removal from water using batch and continuous mode experiments. Optimum removal of Cr(VI) ions was occurred at pH 7. The kinetic results showed that the Cr(VI) removal followed intraparticle diffusion kinetics with a correlation coefficient greater than 0.94. The adsorption isotherms of Cr(VI) could be described very well by both the Langmuir and Freundlich equations (R^2=0.997). The maximum Cr(VI) uptake was found to be 582 µg/g in Langmuir model. Column studies have been carried out to compare these with batch capacities. The Yoon–Nelson and Thomas models were found appropriate for description of the breakthrough curve, whereas the Bohart–Adams model was not match very well. The recovery of Cr(VI) and chemical regeneration of the spent kenaf have also been studied. The high Cr(VI) adsorption capacity and regeneration efficiency of kenaf suggests it as a promising alternative for heavy metal removal specially at near circumneutral pH.

1. Introduction

Nowadays heavy metals are among the most important pollutants in source and treated water, and are becoming a severe public health problem [1]. Chromium (with various oxidation states, *i.e.* Cr(III) and Cr(VI) and Cr(0)) is one of the hazardous heavy metal for biotic and abiotic organisms especially Cr(VI) at concentration higher than 0.05 mg/l act as carcinogenic agent in animals and humans [2]. Cr(VI) attacks kidney, liver and lungs and exhibited carcinogenic properties [3]. Hexavalent chromium (Cr(VI)) is very soluble in water and can form bivalent anions, such as chromate (CrO_4^{2-}), dichromate ($Cr_2O_7^{2-}$), and hydrogen chromate in different pHs, which are much more toxic and hazardous than Cr(III) [4]. Chromium has widespread industrial applications such as chromium plating, wood preservation, textile dyeing and pigmentation, pulp and paper manufacturing, and tanning, which cause large discharge it into the environment [5,6].

In recent years, several methods have been utilized for removal of Cr(VI), including chemical precipitation, electrochemical precipitation, oxidation/reduction, ion exchange, membrane separation, ultrafiltration, flotation, solvent extraction, evaporation, reverse osmosis, foam separation, dialysis/electrodialysis, adsorption and biosorption [7]. Among the mentioned methods, adsorption is an effective and versatile method for removing Cr(VI), particularly when with appropriate regeneration steps are included. However, with regeneration of the adsorbent the problem of sludge disposal will be solved and especially when a low cost adsorbent will be used the process could be economically and environmentally efficient [8]. Several recent publications utilized different low cost and locally abundantly available adsorbents for chromium(VI) removal including treated waste newspaper [9], Melaleuca diosmifolia leaf [10], bio-char [11], wheat bran [12], sugar beet pulp [13] rice bran [14] and Activated carbons [15]. One of the low cost adsorbent is

* Corresponding author: Department of Environmental Health Engineering, Faculty of Public Health, Kermanshah University of Medical Sciences, Kermanshah, Iran. Fax: +98 21 22432037.
E-mail address: anvarasadi@sbmu.ac.ir (A. Asadi).

http://dx.doi.org/10.1016/j.jtice.2016.09.022
1876-1070/

Nomenclature

A	the cross-sectional area of the bed, cm^2
B_{DR}	D–R constant (mol^2/kJ^2)
C_0	the influent concentration, mg/l
C_t	the effluent concentration, mg/l
C_{ad}	the concentration of metal removal, mg/l
E	mean adsorption energy (kJ/mol)
h	initial adsorption rate (mmol/(g•min))
k_1	first-order rate constant of sorption (min^{-1})
k_2	second-order rate constant of sorption (g/µg min)
K_L	Langmuir isotherm constant (l/µg)
K_F	Freundlich constant indicative of the adsorption capacity of the adsorbent (µg/g)
K_{id}	constant of intraparticle diffusion ($g/\mu g\ min^{1/2}$)
k_{Th}	the Thomas model constant, ml/min µg
K_{BA}	Bohart and Adams kinetic constant (l/mg min)
k_{YN}	the rate constant,/min
m_{total}	total amount of metal ion sent to column, mg
N_0	saturation concentration of the bed (mg/l)
Q	the volumetric flow rate, cm^3/min
q_0	the adsorption capacity, µg/g
q_{eq}	equilibrium metal uptake or maximum capacity of the column, µg/g
q_t	amount of adsorbate sorbed on the sorbent surface at any time t (µg/g)
q_{max}	mass of adsorbed solute completely required to saturate a unit mass of adsorbent (µg/g)
q_{total}	the total mass of metal adsorbed, µg
R	universal gas constant, 8.314 (J/(mol•K))
T	absolute temperature (K)
t	the total flow time, min
t_{total}	the total flow time, min
U_0	the superficial velocity, cm/min
V_{eff}	the effluent volume, ml
Z	the bed depth of the fix-bed column, cm
ε	Polanyi potential (J/mol)
τ	the time required for 50% adsorbate breakthrough, min

Kenaf fibers which is an annual dicotyledonous herb in the Malvaceae family and is related to cotton and okra [16]. This plant is easily cultivated and grows well in the tropical regions like many parts of Iran. Kenaf has been used for the adsorption of various pollutants such as basic dye [17], copper (II) [18], nickel [19] and fluoride [20] from aqueous solutions. However, it has not been used for chromium removal yet.

In this study, the Cr(VI) adsorption ability of a low-cost sorbent named Hibiscus Cannabinus kenaf was evaluated. For this, batch and continuous mode sorption experiments were conducted using Hibiscus Cannabinus kenaf as the sorbent. The effects of initial Cr(VI) concentration, pH value and contact time were examined. Attempts have also been made to understand the adsorption kinetics and mechanism of adsorption in both batch and continuous operation. The sorption isotherms were described by using Langmuir and Freundlich isotherm models. The common dynamic models, *i.e.* Yoon–Nelson and Thomas were fitted using nonlinear regression analysis.

2. Materials and methods

2.1. Materials

Dried Hibiscus Cannabinus kenaf fibers as an adsorbent were purchased from local market (Tehran, Iran). Analytical reagent grades of $K_2Cr_2O_7$, NaOH and HCl were supplied by Merck (Germany).

2.2. Preparation of adsorbent

At first, to remove the natural color of kenaf, 250 ml of bleaching solution consisting of 5 wt.% of sodium hypochlorite and sodium hydroxide was added to 5 l of distilled water. Kenaf fibers were cut to length of 1.2 and 1.9 m and immersed in bleaching solution for about 10–15 min at room temperature and then washed with distilled water. After that, to enhance kenaf adsorption capacity, it was soaked in 0.5 M HCl for 30 min and then mercerized by soaking in 0.5 M NaOH for 30 min. finally, kenaf fibers was rinsed with distilled water to obtain effluent pH 7 and dried at 60 °C.

2.3. Batch equilibrium studies

In order to study the effect of different controlling parameters such as pH, initial Cr(VI) concentration, and contact time on Cr(VI) adsorption capacity of kenaf, batch sorption experiments were carried out in 250 ml Teflon flasks. A fixed amount of adsorbent (2 g) was added into 250 ml flask containing 100 ml of Cr(VI) with different concentration (0.5–10 mg/l) and then shaking in a rotary shaker at 100 rpm for 180 min at room temperature (23±2 °C). Adsorption isotherm were carried out with different initial concentrations of Cr(VI) (0.5–10 mg/l) while maintaining the kenaf dosage at a constant level (10 g/l) for 90 min at room temperature. For pH effect, an initial Cr(VI) concentration of 1 mg/l with adsorbent dose of 3 g/l over a pH range of 3–11 were placed in a rotary shaker for 90 min. NaOH (0.1 M) and HCl (0.1 M) were employed to adjust the pH. Samples were withdrawn after a definite time interval and filtered through Whatman No. 1 filter paper (0.45 µm). The residual Cr(VI) analysis was performed with a UV–visible spectrometer (Perkin Elmer Lambda 25 UV/VIS spectrometer; Perkin Elmer, Norwalk, CT, USA) by using diphenyl carbazide as the complexing agent. The absorbance of the pink complex formed solution was read at 540 nm [21]. The uptake (q) of Cr(VI) expressed as Cr(VI) removal per unit mass of kenaf (µg Cr/g) at time t was calculated using Eq. (1)

$$q_t = \frac{(C_0 - C_t)V}{m} \quad (1)$$

Where C_0 and C_t are the Cr(VI) initial and equilibrium concentration (mg/l) at time t, V is the solution volume (l), and m is the adsorbent mass (g). All experiments were conducted in triplicate.

2.4. Regeneration of kenaf

To recover the adsorbed Cr(VI) and to regenerate the adsorbent as an important issue for further use desorption studies were carried out. After saturation, the kenaf was washed with NaOH (0.5 M) and HCl (0.5 M) each for 30 min. simultaneously, the regenerated adsorbent was also used and they results were compared.

2.5. Fixed-bed column studies

The fixed-bed column studies were carried out in a column made up Pyrex glass with 0.55 cm internal diameter and a total length of 25 cm. A known quantity of the Hibiscus Cannabinus was packed in the column to yield the bed mass of 2.2 g and effective depth of 15 cm. The inert beads were placed at the bottom and top of the adsorbent. The bed volume was calculated to be 6 ml and column was operated in a down flow mode. At first, deionised water was passed through the column, and then, Cr(VI) solution with known initial concentration (0.5 mg/l) at pH 7.0 (optimum pH for removing Cr(VI) using kenaf) at a fixed flow rate (2.2 ml/min)

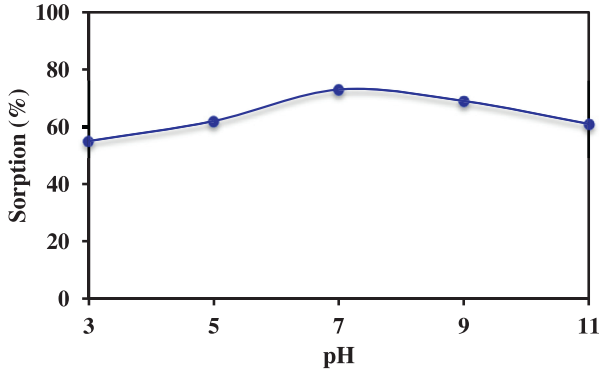

Fig. 1. Effect of pH on the removal of chromium by Hibiscus Cannabinus kenaf. Conditions: Cr(VI) =1 mg/l; Kenaf dosage =3 g/l; equilibration time =90 min.

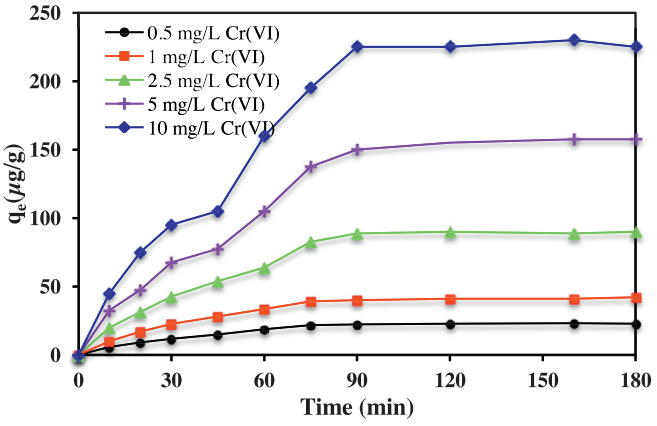

Fig. 2. Effect of agitation time on the adsorption of Cr(VI) onto kenaf.

was passed through the bed (Empty Bed Contact Time = 2.96 min). The passing of chromium solution in the bed was continued until there was no further adsorption. Samples were collected at various time intervals and analyzed for residual Cr(VI) concentration.

3. Results and discussion

3.1. Effect of pH

The initial solution pH has an important effect on Cr(VI) adsorption because the pH of an aqueous medium will control the magnitude of the electrostatic charges that influences on cation and anion sorption from solution to the adsorbent [17]. The effect of pH was investigated for Cr(VI) adsorption at an initial Cr(VI) concentration of 1 mg/l with adsorbent dose of 3 g/l over a pH range of 3–11. The effect of pH is presented in Fig. 1, which shows the maximum adsorption was obtained at a pH of *ca.* 7 (73%), with decreasing values on either side of this pH. The effect of pH on the adsorption of metal is greatly related to the two main factors: the chemistry of metal in solution and type and ionic state of the functional group present in the adsorbent [22]. At acidic pH, the predominant species of Cr are $Cr_2O_7^{2-}$, $HCrO_4^-$,$Cr_3O_{10}^{2-}$ and $Cr_4O_{13}^{2-}$ and at pH 8 CrO_4^{2-} is stable and at pH range 3–6, the equilibrium shifts to dichromate according to the following equation [23, 24]:

$$2CrO_4^{2-} + 2H^+ \rightarrow Cr_2O_7^{2-} + H_2O \quad (2)$$

On the other hand, the pH_{zpc}(zero point of charge) of the adsorbent is at 7.1 which below this pH, the surface charge of the adsorbent is positive and above this pH the surface charge becomes negative. Thus, at pH lower than pH_{zpc}, the surface of the adsorbent becomes favors for the uptake of Cr(VI) in the anionic form. With increase in pH, the electrostatic repulsion between negatively adsorbent surface and the anionic form of Cr(VI) increased and as well as competition between OH^- and chromate ions (CrO_4^{2-}) increased, which lead to gradually decrease in adsorption. At highly acidic pH, there is a possibility that Cr(VI) is reduced to Cr(III), which Cr(III) is weakly adsorbed in a lower pH range [25]. Similar results were reported in the literature for the adsorption of basic dye using acid treated kenaf fiber [17] and floride adsorption using modified kenaf [20]. Attaining the highest adsorption of Cr(VI) at near circumneutral pH is great importance for full scale application, because the pH of natural water is usually neutral, thus it does not require pH adjustment before treatment.

3.2. Adsorption kinetics

The effect of contact time was evaluated in batch study containing 100 ml of different initial Cr(VI) concentration, 2 g adsorbent and initial pH of 7. Batch sorption kinetics is necessary for the design of fixed bed column. Adsorption kinetics was studied for describing the rate of Cr(VI) ion adsorption, mechanism of adsorption, possible rate-controlling steps and evaluation the utility of adsorbent for metal removal [26,27]. The effect of contact time on Cr(VI) sorption capacity is shown of Fig. 2. It can be seen that q_e increases rapidly in first 30 min of adsorption and then further increases at a relatively slow rate at next 30 min, and finally reaches equilibrium after approximately 90 min and after that no increase in q_e was observed. These adsorption data were analyzed and simulated using four kinetic models including the pseudo-first-order, pseudo-second-order, intra-particle diffusion and Elovich models.

3.3. Lagergren pseudo-first-order and pseudo-second order kinetics

The pseudo-first-order and pseudo-second order kinetic models are used commonly for determining the adsorption rate and analysis adsorption process. The linear forms of these equations are expressed as following:

$$\log(q_e - q_t) = \log q_e - \frac{k_1 t}{2.303} \quad (3)$$

$$\frac{t}{q_t} = \frac{1}{k_2 q_e^2} + \frac{t}{q_e} \quad (4)$$

where q_t and q_e (μg/g) are the adsorption capacity of kenaf in any time (t) and equilibrium; K_1 (min^{-1}) is the rate constant of the pseudo-first-order model; and K_2 (g/μg min) is the rate constant of the pseudo-second-order model. The experimental data in Fig. 2 were fitted with the linear form using Eqs. (3) and (4) and results are shown in Fig. 3a and b, respectively. The obtained kinetic parameters are presented in Table 1. The value of correlation coefficient (R^2) for Lagergren pseudo-first-order model was relatively low and the theoretical q_e was not agreed well with experimental. These results indicated that Cr(VI) adsorption on kenaf does not followed the pseudo-first-order. The values of k_2 and $q_{e2,\ theor}$ of the pseudo-second-order model were calculated from the intercept and slope of straight line plots of t/q_t versus t (Fig. 3b) and presented in Table 1. The calculated correlation coefficients (R^2) were relatively high and theoretical q_e were agreed well with the experimental equilibrium amounts. However, the small difference between the theoretical and experimental values of q_e may relate to the uncertainty inherent in obtaining the experimental q_e values. This suggests that the adsorption of Cr(VI) onto kenaf is highly controlled by the chemisorption behavior probably related to exchange or sharing of electrons between cation groups of kenaf and anion groups of chromium(VI) [27,28]. The increased in

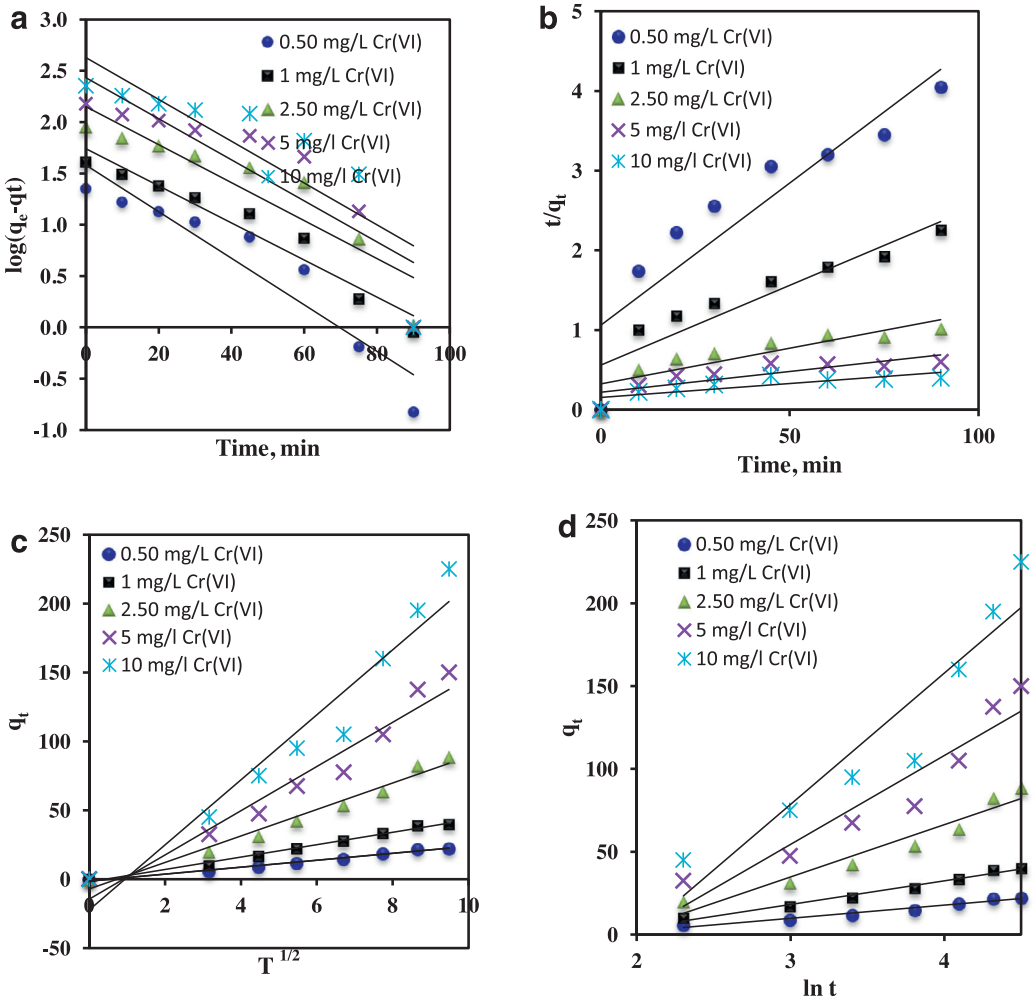

Fig. 3. Kinetic plots for Cr(VI) adsorption (a) pseudo-first-order (b) pseudo-second-order (c) Intra-particle model (d) Elovich model.

Table 1
Kinetic parameters for adsorption of Cr(VI) on kenaf.

C_0 (mg/l)	$q_{e\ (exp)}$ (μg/g)	Pseudo-first-order model			Pseudo-second-order model			
		$K_1\times10^{-2}$	$q_{e\ (theor)}$	R^2	$K_2\times10^{-4}$	$q_{e\ (theor)}$	h	R^2
0.5	21.8	5.2	38.2	0.882	10	28	0.94	0.827
1	39.1	4.1	55	0.942	7	50	1.8	0.85
2.5	82.6	4.2	141	0.834	2	112	3.1	0.756
5	137.6	4.6	270	0.774	1	193	4.5	0.672
10	195.1	4.7	425	0.710	0.7	286	6.5	0.638

C_0 (mg/l)	$q_{e\ (exp)}$ (μg/g)	Intraparticle diffusion model			Elovich model		
		K_{id}	C	R^2	α	β	R^2
0.5	21.8	2.5	1.3	0.940	1.4	0.13	0.963
1	39.1	4.5	2	0.949	2.5	0.07	0.982
2.5	82.6	9.2	7.1	0.972	4.7	0.03	0.938
5	137.6	16	14.5	0.989	7.3	0.02	0.897
10	195.1	23. 5	22.3	0.984	10.6	0.01	0.883

q_e with increasing of initial Cr(VI) concentration may related to decreased in mass transfer resistance of pollutant from bulk solutions to adsorbent surface. The initial sorption rate (h) was calculated from the following relation [29]:

$$h = k_2 q_e^2 \quad (5)$$

where h is the initial sorption rate (μg/g min). From Table 1, it was observed that initial sorption rate increased and pseudo-second-order-rate constant K_2 decreased with increase in initial Cr(VI) concentration. This indicated that the mass transfer rate of pollutant improved with increase in initial Cr(VI) concentration [30].

3.4. Intra-particle diffusion model

The intra-particle diffusion rate was used for further mechanism of the Cr(VI) adsorption onto kenaf because its important rate-limiting step especially when the process are carried out as

batch operation mode [29]. The equation is expressed as follow:

$$q_t = k_{id} t^{0.5} + C \quad (6)$$

where k_{id} is intra-particle diffusion rate constant (μg/g $min^{0.5}$), q_t is the amount of Cr(VI) adsorbed at any time t (μg/g) and C is a constant related to the extent of the boundary layer effect. The amount of k_{id} was obtained from the slope of the linear plot of q_t versus t. As can be seen in Fig 3c, the plots were almost pass through the origin (0,0) which indicated that the species diffusion are the involved mechanism of adsorption and slop of linear curves are the diffusion rate constants (k_{id}) [31]. The intra-particle diffusion model had the highest coefficients ($R^2 > 0.94$), which suggested that the adsorption of Cr(VI) on kenaf was predominantly intra-particle diffusion. Furthermore, the highest values of k_{id} between the kinetic models was related to the higher swelling ratio of the adsorbent, resulting in the formation of larger surface area for Cr(VI) diffusion [27]. However, in a system with good mixing, large particle sizes of adsorbent and low affinity between adsorbate and adsorbent, the intra-particle diffusion will control the sorption process [32].

3.5. Elovich model

The Elovich kinetic equation, was used at first for describing of gas adsorption phenomenon, nowadays is widely used to depict the aqueous contaminants sorption by assuming strong heterogeneity of sorbent surface which is based on general second-order-reaction mechanism [33]. The Elovich equation is expressed as follow:

$$q_t = \frac{1}{\beta} \ln(\alpha\beta) + \frac{1}{\beta} \ln t \quad (7)$$

where α (μg/g.min) is the initial adsorption rate and β (g/μg) is the sorption constant and is related to the surface coverage and the activation energy for the chemical adsorption. These constants can be calculated from the slop and intercept of the linear plot of q_t versus ln t [34]. The Elovich equation of q_t versus ln t is shown on Fig. 3d. The values of α, β and R^2 are presented in Table 1. The experimental data had a good fit with the Elovich equation as indicated by R^2 values of 0.877–0.976. The initial adsorption rate (α) was increased with increasing initial Cr(VI) concentration. This implies the predominance of Cr(VI) adsorption on kenaf with assuming a multilayer adsorption, which every layer shows various activating energy for chemisorptions [33].

3.6. Sorption equilibrium

Generally, an adsorption isotherm is an inestimable curve describing the phenomenon governing the retention (or release) or mobility of a compound from the aqueous porous media or aquatic environments to a solid particles at a constant temperature and pH [35,36]. Adsorption equilibrium (the ratio between the adsorbed amounts with the value remaining in the solution) is based on adsorbing of solid phase onto the adsorbent for sufficient time, when adsorbate concentration in the bulk solution is in a dynamic balance with the interface concentration [35,37]. To describe, the interaction between chromium(VI) molecules and kenaf surface, the experimental equilibrium data were fitted with several models. To optimizing the adsorption process, identifying of the best isotherm model is a critical issue. For this purpose, Langmuir, Freundlich and Dubinin–Radushkevich (D–R) isotherm models were implemented to the batch equilibrium data.

3.6.1. Langmuir isotherm

Langmuir adsorption equation was originally developed to describe gas–solid phase adsorption onto activated carbon. It was based on three assumptions: (i) the adsorption sites are identical, (ii) the adsorption is limited to a finite (fixed) number of definite localized sites and (iii) all sites are energetically and sterically independent of the adsorbed quantity [36,38]. The linear form of the isotherm is as follow:

$$\frac{1}{q_e} = \left(\frac{1}{K_L q_{max}}\right)\frac{1}{C_e} + \frac{1}{q_{max}} \quad (8)$$

where q_{max} (μg/g) is maximum adsorption capacity and K_L is related to adsorption energy (l/μg). The amount of q_{max} and K_L can be calculated from the intercept and slop of $1/q_e$ versus $1/C_e$ plot (Fig. 4a). The values of q_{max} and K_L for the adsorption of Cr(VI) on kenaf are listed in Table 2.

The essential characteristics of the Langmuir isotherm which classified by a term R_L, dimensionless constant separation factor or equilibrium parameter, is necessary for determining whereas adsorption is favorable or unfavorable. R_L is defined as below [31,35]:

$$R_L = \frac{1}{1 + K_L C_0} \quad (9)$$

where R_L is separation factor (dimensionless), K_L is Langmuir constant and C_0 (μg/l) is the initial concentration of the adsorbate. The lower value of the R_L reflects that the adsorption is favorable. In a deeper interpretation, R_L value indicates the adsorption nature to be either unfavorable ($R_L > 1$), linear ($R_L = 1$), favorable ($0 < R_L < 1$) or irreversible ($R_L = 0$). The value of R_L presented in Table 2, indicated that the adsorption behavior of Cr(VI) onto kenaf is favorable ($0 < R_L < 1$). The adsorption capacity of Cr(VI) onto Hibiscus Cannabinus kenaf was compared with other low cost adsorbents and listed in Table 3.

Table 2
Constant parameters and correlation coefficients calculated for various adsorption models for Cr(VI) onto kenaf.

Isotherm models	Parameters			R^2
Langmuir	q_{max}	K_L	R_L	
	582.3	0.06	0.001	0.997
Freundlich	K_F	n	$\Delta\Gamma$	
	36	1	−25	0.997
D–R	B_{DR}	Q_m	E	
	-6.5×10^{-8}	32	2.76	0.919

3.6.2. Freundlich isotherm

Freundlich isotherm model is another common model which is originally empirical in nature and describing the non-ideal and reversible adsorption process. If the adsorption sites are more than pollutant molecules then Freundlich isotherm can be used for describing of just physical adsorption process. In contrary with monolayer Langmuir model, Freundlich model is a multilayer model which does not predict any saturation of the sorbent by sorbate [46]. It can be expressed in the following linear form:

$$\log q_e = \log k_F + \frac{1}{n} \log C_e \quad (10)$$

Freundlich isotherm is generally used in special cases for heterogeneous surface energy where it is characterized by the heterogeneity factor $1/n$. K_F (μg/g(L/mg)$^{1/n}$) and n are Freundlich constants which indicate sorption capacity and intensity, respectively and calculated from the intercepts and slopes of the Freundlich plots of log q_e against log C_e (Fig. 4b). According to Table 2, the n value is equal to unit which n value between 0 and 10 indicate the beneficial adsorptions [47]. The free energy change (ΔG) of Cr(VI) adsorption onto kenaf with knowing the K_F amount, can be obtained through following equation:

$$\Delta G = -RT \ln(K_F \times 1000) \quad (11)$$

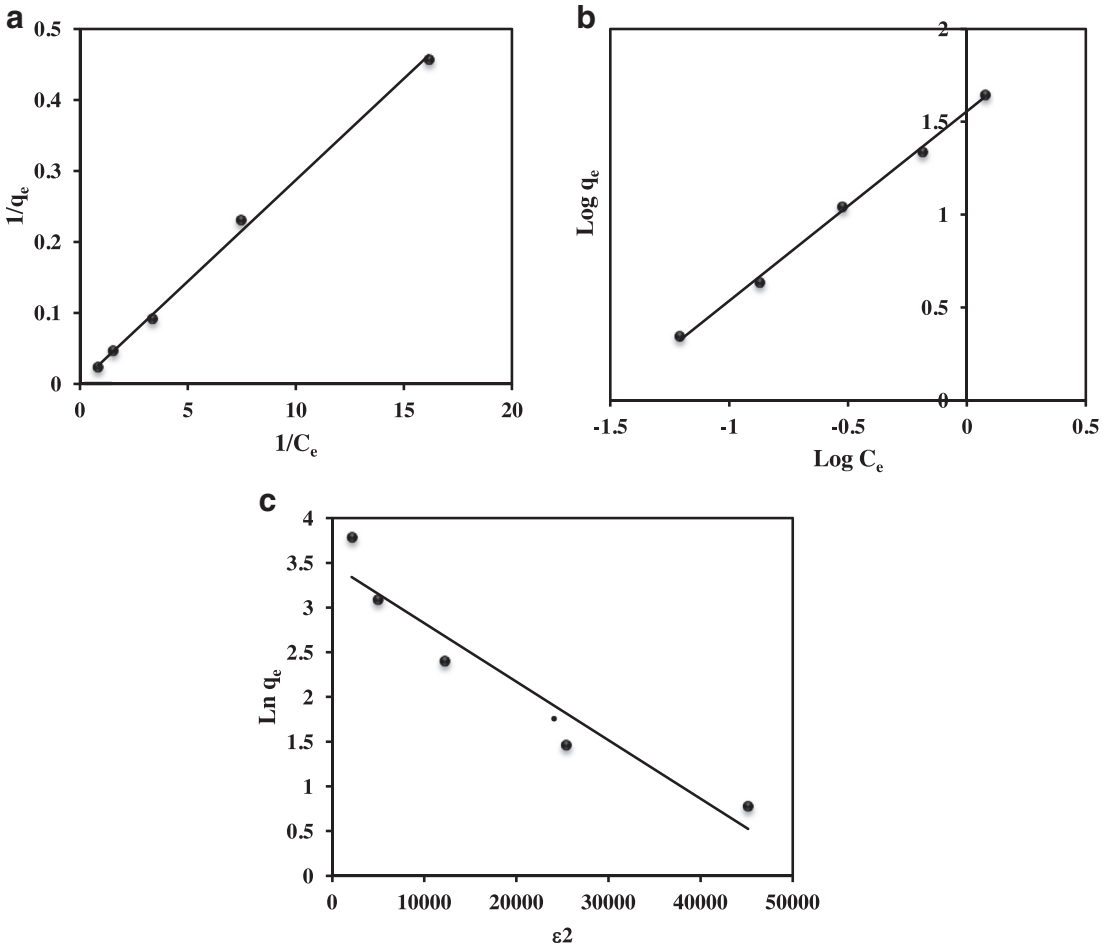

Fig. 4. Adsorption isotherm models of Cr(VI) on kenaf (a) Langmuir and (b) Freundlich and (c) Dubinin–Radushkevich models.

Table 3
Comparative evaluation of Langmuir adsorption capacities of kenaf vis other low cost adsorbent for Cr(VI) removal.

Adsorbents	pH	Temp. (°C)	Adsorption capacity (mg/g)	Reference
Raw rice bran	5.0	25	0.07	[14]
Palygorskite clay	7.0	25	58.5	[39]
Maghemite nanoparticles	8.0	22.5	1.9	[40]
Coconut shell charcoal	6.0	29	9	[41]
Bauxite	2.0	20	0.5	[42]
Modified oak sawdust	3.0	20	1.7	[43]
Pinus brutia	2.0	40	69.4	[24]
Oak wood char	2.0	25	3.03	[11]
Activated slog	1.0	30	1.41	[44]
Turkish coffee	6.0	Room temperature	1.63	[45]
Hibiscus Cannabinus Kenaf	7	Room temperature	0.582	Present study

where R is the gas constant (0.00831447 kJ/K mol) and T is the temperature (293 K). The negative free energy values (Table 2) indicated that the adsorption process is spontaneous and feasible. Base on correlation coefficient (R^2 = 0.997), the adsorption of Cr(VI) onto kenaf followed both the Langmuir and Freundlich equations very well.

3.6.3. Dubinin–Radushkevich (D–R) isotherm model

The constants of Langmuir and Freundlich isotherms did not provide anything about mechanism of adsorption. For that reason, for explaining the adsorption type and mechanism, the equilibrium data were fitted and described by D–R isotherm model [48]. It can be expressed in the following linear form:

$$\ln q = \ln Q_m - B_{DR}\varepsilon^2 \quad (12)$$

Where ε (Polanyi potential)$=RT \ln (1+1/C_e)$, q is amount of Cr(VI) adsorbed on unit mass of adsorbent (μg/g), Q_m is the maximum amount of adsorbed Cr(VI) under the optimum condition and B_{DR} (mol^2/kJ^2) is constant with a dimension of energy. The parameters Q_m and B_{DR} obtained from the intercept and slope of ln q versus ε^2 (Fig. 4c and Table 2). The mean energy of sorption, E, is calculated as following:

$$E = \frac{1}{\sqrt{-2B_{DR}}} \quad (13)$$

The magnitude of E is used to express the type of sorption reaction (physical or chemical). When E parameter is less than 8 kJ/mol, the adsorption process has physical in nature. The E value obtained

was around 2.76 kJ/mol, indicated physisorption due to the weak van der waals forces [48,49].

3.7. Column studies

3.7.1. Breakthrough analysis

The high chromium adsorption capacity of Hibiscus Cannabinus kenaf has been demonstrated in the batch experiments. To evaluate the column performance for Cr(VI) adsorption by kenaf, the continuous flow experiments were carried out. In the continuous flow, at first, the adsorbent at the top of a column saturates and maximum removal takes place initially. The adsorption zone moves down ward with passing time and reaches the exit of the bed, which at this time the concentration of the adsorbate in the effluent becomes equal to the influent. A plot of effluent and influent concentration ratios (C_t/C_0) versus effluent volumes (V) or elapse time (t) is known as breakthrough curve. The shape and volume of breakthrough curve are very important parameters for determining the operation and the dynamic conditions of an adsorption column [50]. The recommended limit of Cr(VI) in drinking water is 0.05 mg/l [51] and therefore in this study breakthrough point time was defined as the time when the Cr(VI) concentration in the outlet reaches 0.05 mg/l. The column capacity at the breakthrough point is determined from the following equation:

$$q_b = \frac{C_0}{m}\int_0^{V_b}\left(1-\frac{C_t}{C_0}\right)dV \tag{14}$$

where q_b is the column capacity at breakthrough point (mg/g), m is the adsorbent mass (g), C_0 and C_t are the initial and effluent adsorbate concentration (mg/l), respectively, and V_b is the volume processed at breakthrough point (l). The number of bed volumes (BV) processed before the breakthrough point is an important parameter in evaluation of adsorbent performance and BV is used in total cost of fixed bed [52]. The number of bed volumes (BV) is defined by the following:

$$\text{number of bed volumes (BV)} = \frac{\text{volume of water treated at breakthrough point, ml}}{\text{volume of adsorbent bed, ml}} \tag{15}$$

Adsorbent exhaustion rate (AER) is another bed performance indicator which is used in the operating costs of the adsorbent column [52]. AER is defined as the mass of adsorbent deactivated per volume of liquid treated at breakthrough which is given by the following:

$$\text{adsorbent exhaustion rate (AER)} = \frac{\text{mass of adsorbent in column, g}}{\text{volume treated at breakthrough, ml}} \tag{16}$$

The breakthrough curve of Cr(VI) adsorption by Hibiscus Cannabinus kenaf at fixed flow rate of (2 ml/min) and at fixed bed height of 15 cm is shown in Fig. 5. The volumes of water processed (V_b) at breakthrough point was 45 ml and the number of bed volumes (BV) processed at this point was 13. The breakthrough capacity (q_b) was found to be 9.2 μg/g at empty bed contact time of 2.96 min. It is evident from Fig. 5 that the breakthrough curve was not very steep which means that the exhaustion of the bed was not very fast. Total adsorbed Cr(VI) (q_{total}; μg) in the column for a given influent concentration and flow rate is calculated from the following:

$$q_{total} = \frac{QA}{1000} = \frac{Q}{1000}\int_{t=0}^{t=\text{total}} C_{ad}\,dt \tag{17}$$

Which A is area under the breakthrough curve of adsorbate concentration (C_{ad}) versus flow time (t) [53].

Table 4
Yoon–Nelson, Thomas and Bohart–Adams models parameters for adsorption of Cr(VI) onto kenaf in a fixed-bed column.

Yoon–Nelson model			Thomas model			Bohart–Adams model		
K_{YN}	τ	R^2	K_{TH}	q_0	R^2	K_{BA}	N_0	R^2
0.085	27.2	0.959	0.17	21.48	0.959	0.068	9.75	0.772

The total amount of inlet Cr(VI) ion to the column (m_{total}) was calculated from the following equation [54]:

$$m_{total} = \frac{QC_0t_{total}}{1000} \tag{18}$$

Total Cr(VI) removal was obtained from the ratio of total amount of adsorbed Cr(VI) to total inlet Cr(VI) ion to the column as following equation [55]:

$$\text{Total removal}(\%) = \frac{q_{total}}{m_{total}} \times 100 \tag{19}$$

Equilibrium adsorption studies provide information about the amount of required adsorbent to adsorb a unit mass of contaminant under the flow through condition. Equilibrium adsorption (q_{eq}) is defined by Eq. (20) as the total amount of Cr(VI) sorbed per g of sorbent (X) at the end of total flow time.

$$q_{eq} = \frac{q_{total}}{X} \tag{20}$$

In this study, the values of q_{total}, m_{total}, Total removal, and q_{eq} at fixed influent concentration (C_0) of the feed (0.5 mg/l) and fixed flow rate (2 ml/min) were 0.0466 mg, 0.09 mg, 52% and 21 μg/g, respectively. The equilibrium adsorption capacities of the Hibiscus Cannabinus kenaf in column and batch experiments for the same initial Cr(VI) concentration (0.5 mg/l) are equal. This may due to reason that the pores of the Hibiscus Cannabinus kenaf favor improved solid state diffusion in fixed bed column as same as batch operation [56]. In this study, three mathematical models; Yoon–Nelson, Thomas and Bohart–Adams were used to match the experimental data of breakthrough behaviors of Cr(VI) adsorption onto kenaf and model data.

3.7.2. The Yoon–Nelson model

The Yoon–Nelson's model is a relatively simple model that is based on the adsorption of vapors or gases on solid sorbents such as activated coal [57]. This model is based on the assumption that the rate of decrease in the probability of adsorption for each adsorbate molecule is proportional to the probability of adsorbate adsorption and the probability of adsorbate breakthrough on the adsorbent [57]. The Yoon–Nelson model for a single component system can be expressed as:

$$\frac{C_t}{C_0 - C_t} = \exp\left(K_{YN}t - \tau K_{YN}\right) \tag{21}$$

where k_{YN} is the rate constant (min^{-1}) and τ is the time required for 50% adsorbate breakthrough (min). A linear plot of $\ln[C_t/(C_0 - C_t)]$ against t determined the values of k_{YN} and τ from the intercept and slope of the plot (plot not shown). The fitted breakthrough curves by the Yoon–Nelson model is shown in Fig. 5. The Yoon–Nelson model rate constant (k_{YN}), the correlation coefficient R^2 and the value of τ calculated is presented in Table 4. The R^2 value is 0.959 which indicated that the Yoon–Nelson model is highly valid for Cr(VI) adsorption by Hibiscus Cannabinus kenaf and closely represents the experimental breakthrough curve.

3.7.3. The Thomas model

Thomas model assumes plug flow behavior in the column and was used to assess the capacity of the adsorbent in a fixed bed

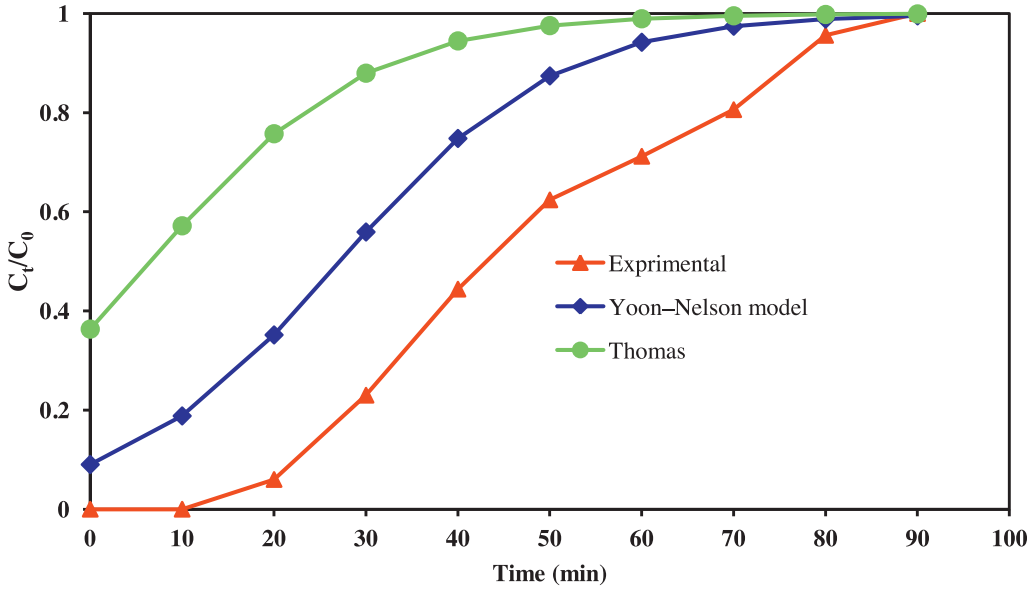

Fig. 5. Comparison of the experimental and predicted breakthrough curve according to the Yoon–Nelson and Thomas models. Conditions: flow rate =2 ml/min; bed mass = 2.2 g; initial Cr(VI) concentration =0.5 mg/l.

column [58]. The Thomas model is based on the following assumption: (i) the mass transfer at the interface limited the adsorption process and it is not limited by chemical interactions and (ii) the process data follows Langmuir isotherms and second-order kinetics [59]. The maximum adsorption capacity of the column could be calculated by Thomas model. The equation of the Thomas model could be expressed as follows:

$$\frac{C_t}{C_0} = \frac{1}{1 + \exp\left(\frac{k_{TH} q_0 m}{v} - k_{TH} C_0 t\right)} \tag{22}$$

where k_{Th} is Thomas rate constant (ml/min mg); q_0 is equilibrium adsorption capacity (mg/g); m is the amount of absorbent in the column (g); C_0 and C_t are the Cr(VI) concentration in the influent and at time t, respectively (mg/l); v is the flow rate (ml/min). The values of k_{TH} and q_0 as determined from slope and intercept of the plot (plot not shown) of ln $(C_0/C_t - 1)$ versus time flow (t). The fitted breakthrough curves by the Thomas model is shown in Fig. 5. The Thomas parameters were calculated by linear regression analysis and are shown in Table 4. The R^2 value is 0.959 which indicated that the Thomas model is also highly valid for Cr(VI) adsorption. The q_0 value (21.48 μg/g) is completely in consistent with the experiment value $q_{eq(exp)}$ (21 μg/g). This may be due to it closely agreement with the Langmuir thermodynamics equation [60] and good kinetics [61] for Cr(VI) adsorption on Hibiscus Cannabinus kenaf. Based on R^2 values comparison, both the Yoon–Nelson and Thomas models could be applied to predict adsorption performance for adsorption of Cr(VI) in a fixed-bed column and this results are in agreement with Chen et al. [7]. On the other hand, the Bohart and Adams model was not enough match with experimental adsorption data (R^2= 0.77) (data were not shown for Bohart and Adams model).

3.8. Desorption of Cr(VI) and regeneration of the adsorbent

Sorption of solute on the adsorbent can occur via physical bonding, ion-exchange or combination of both. In case of sorption by chemical bonding or ion-exchange or combination of the both, the solute can be desorbed effectively by strong desorbents like acid or alkali solutions. Desorption of Cr(VI) from adsorbent is very important in view of industrial applications. In this study, Cr(VI) desorption was performed using 0.5 M NaOH and 0.5 M HCl solutions in batch mode for 30 min. It was observed that 100 ml of 0.5 M HCl was sufficient for 92% Cr(VI) desorption for the mentioned contact time (Fig. 6). However, at the same conditions, about 88% Cr(VI) was desorbed for 0.5 M NaOH. After desorption and rising the adsorbent with distilled water, the adsorbent was used for adsorption of Cr(VI) with different initial concentration (0.5–10 mg/l) at equilibrium time and results are shown in Fig. 6. As can be seen, acid washing was better than base washing and the sorption Cr(VI) was found to be 89 and 45% for initial concentration of 0.5 and 10 mg/l in first use and was 87 and 35% for initial concentration of 0.5 and 10 mg/l in 2nd use acid washing, respectively. Desorption of Cr(VI) from Cr(VI) laden *Tamarindus indica* seeds (TS) was more favored by NaOH than distilled water and HCl [62]. The adsorption capacity decreases slightly in the 2nd use especially in higher initial concentration when compared with the

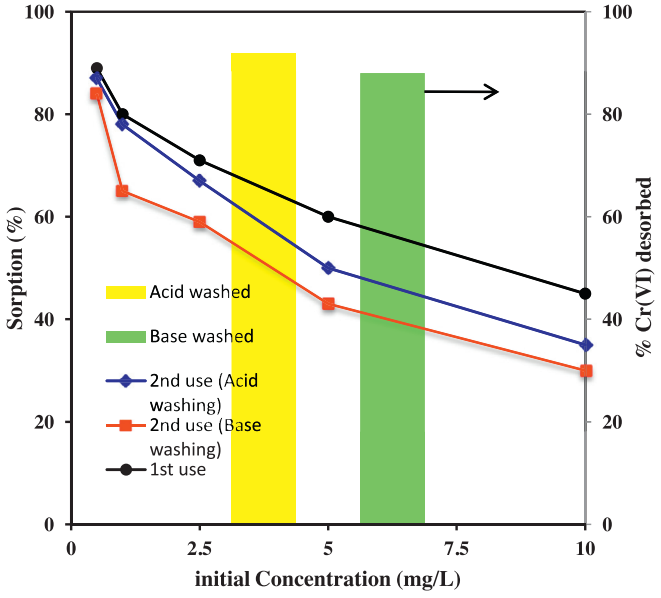

Fig. 6. Comparison of the acid and base washing on the % Cr(VI) desorption from kenaf and regeneration efficiency.

first cycle. Similar results were observed for the adsorption of Cr^{6+} and pb^{2+} by red mud [56] and Cr(VI) adsorption on crosslinked chitosan–Fe(III) complex [50].

4. Conclusions

This study deal with the adsorption of Cr(VI) on Hibiscus Cannabinus kenaf from aqueous solutions using batch and continuous mode experiments. This kenaf can be used as an effective and low cost adsorbent for the removal of Cr(VI) ions from aqueous solutions. The following conclusions were drawn from the results of this study:

- Hibiscus Cannabinus kenaf was used with a facile activation treatment which decreases the sorption costs.
- The maximum adsorption capacity ($q_{max} = 582\,\mu g/g$) was observed at near circumneutral pH (pH $\cong$ 7).
- The adsorption of Cr(VI) on kenaf reached equilibrium at 90 min contact time.
- The adsorption kinetic was described well by the intraparticle diffusion model, indicating that the adsorption process is almost intraparticle diffusion and intraparticle diffusion is the rate controlling step of the adsorption process.
- The equilibrium data fitted well to the both Langmuir and Freundlich isotherm models.
- Based on R^2 values comparison, both the Yoon–Nelson and Thomas models could be applied to describe well the experimental breakthrough curve for the adsorption of Cr(VI) in a fixed-bed column.
- The spent adsorbent can be chemically regenerated very well by treating it with 0.5 M HCl.

References

[1] Demirbas A. Heavy metal adsorption onto agro-based waste materials: a review. J Hazard Mater 2008;157:220–9.
[2] Dehghani MH, Heibati B, Asadi A, Tyagi I, Agarwal S, Gupta VK. Reduction of noxious Cr(VI) ion to Cr(III) ion in aqueous solutions using H_2O_2 and UV/H_2O_2 systems. J Ind Eng Chem 2016;33:197–200.
[3] Narin I, Soylak M, Kayakirilmaz K, Elci L, Dogan M. Speciation of Cr(III) and Cr(VI) in tannery wastewater and sediment samples on Ambersorb 563 resin. Anal Lett 2002;35:1437–52.
[4] Golestanifar H, Haibati B, Amini H, Dehghani MH, Asadi A. Removal of hexavalent chromium from aqueous solution by adsorption on γ-Alumina nanoparticles. Environ Prot Eng 2015;41:133–45.
[5] Assadi A, Dehghani MH, Rastkari N, Nasseri S, Mahvi AH. Photocatalytic reduction of hexavalent chromium in aqueous solutions with zinc oxide nanoparticles and hydrogen peroxide. Environ Prot Eng 2012;38:5–16.
[6] Dakiky M, Khamis M, Manassra A, Mer'eb M. Selective adsorption of chromium (VI) in industrial wastewater using low-cost abundantly available adsorbents. Adv Environ Res 2002;6:533–40.
[7] Chen S, Yue Q, Gao B, Li Q, Xu X, Fu K. Adsorption of hexavalent chromium from aqueous solution by modified corn stalk: a fixed-bed column study. Bioresour Technol 2012;113:114–20.
[8] Bailey SE, Olin TJ, Bricka RM, Adrian DD. A review of potentially low-cost sorbents for heavy metals. Water Res 1999;33:2469–79.
[9] Dehghani MH, Sanaei D, Ali I, Bhatnagar A. Removal of chromium(VI) from aqueous solution using treated waste newspaper as a low-cost adsorbent: kinetic modeling and isotherm studies. J Mol Liq 2016;215:671–9.
[10] Kuppusamy S, Thavamani P, Megharaj M, Venkateswarlu K, Lee YB, Naidu R. Potential of Melaleuca diosmifolia leaf as a low-cost adsorbent for hexavalent chromium removal from contaminated water bodies. Process Saf Environ Prot 2016;100:173–82.
[11] Mohan D, Rajput S, Singh VK, Steele PH, Pittman Jr CU. Modeling and evaluation of chromium remediation from water using low cost bio-char, a green adsorbent. J Hazard Mater 2011;188:319–33.
[12] Dupont L, Guillon E. Removal of hexavalent chromium with a lignocellulosic substrate extracted from wheat bran. Environ Sci Technol 2003;37:4235–41.
[13] Altundogan HS. Cr(VI) removal from aqueous solution by iron (III) hydroxide-loaded sugar beet pulp. Process Biochem 2005;40:1443–52.
[14] Oliveira EA, Montanher SF, Andrade AD, Nóbrega JA, Rollemberg MC. Equilibrium studies for the sorption of chromium and nickel from aqueous solutions using raw rice bran. Process Biochem 2005;40:3485–90.
[15] Mohan D, Pittman Jr CU. Activated carbons and low cost adsorbents for remediation of tri- and hexavalent chromium from water. J Hazard Mater 2006;137:762–811.
[16] Gharehchahi E, Mahvi AH, Shahri SMT, Davani R. Possibility of application of kenaf fibers (Hibiscus cannabinus L.) in water hardness reduction. Desalin Water Treat 2014;52:6257–62.
[17] Mahmoud DK, Salleh MAM, Karim WAWA, Idris A, Abidin ZZ. Batch adsorption of basic dye using acid treated kenaf fibre char: equilibrium, kinetic and thermodynamic studies. Chem Eng J 2012;181–182:449–57.
[18] Hasfalina C, Maryam R, Luqman C, Rashid M. Adsorption of copper (II) from aqueous medium in fixed-bed column by kenaf fibres. APCBEE Procedia 2012;3:255–63.
[19] Florence JAK, Gomathi T, Thenmozhi N, Sudha PN. Adsorption study: removal of nickel ions using Kenaf fiber/chitosan biosorbent. J Chem Pharm Res 2015;7:410–22.
[20] Yusof S, Zahra N, Koay Y, Nourouzi M, Chuah L, Choong T. Removal of fluoride using modified kenaf as adsorbent. J Eng Sci Technol 2015;10:11–22.
[21] Hosseini-Bandegharaei A, Hosseini MS, Sarw-Ghadi M, Zowghi S, Hosseini E, Hosseini-Bandegharaei H. Kinetics, equilibrium and thermodynamic study of Cr(VI) sorption into toluidine blue o-impregnated XAD-7 resin beads and its application for the treatment of wastewaters containing Cr(VI). Chem Eng J 2010;160:190–8.
[22] Gupta VK, Shrivastava AK, Jain N. Biosorption of Chromium(VI) from aqueous solutions by green algae spirogyra species. Water Res 2001;35:4079–4085.
[23] Mor S, Ravindra K, Bishnoi NR. Adsorption of chromium from aqueous solution by activated alumina and activated charcoal. Bioresour Technol 2007;98:954–7.
[24] Ozdes D, Gundogdu A, Kemer B, Duran C, Kucuk M, Soylak M. Assessment of kinetics, thermodynamics and equilibrium parameters of Cr(VI) biosorption onto Pinus brutia Ten. Can J Chem Eng 2014;92:139–47.
[25] Rengaraj S, Joo CK, Kim Y, Yi J. Kinetics of removal of chromium from water and electronic process wastewater by ion exchange resins: 1200H, 1500H and IRN97H. J Hazard Mater 2003;102:257–75.
[26] Sari A, Tuzen M. Cd(II) adsorption from aqueous solution by raw and modified kaolinite. Appl Clay Sci 2014;88–89:63–72.
[27] Zhou C, Wu Q, Lei T, Negulescu II. Adsorption kinetic and equilibrium studies for methylene blue dye by partially hydrolyzed polyacrylamide/cellulose nanocrystal nanocomposite hydrogels. Chem Eng J 2014;251:17–24.
[28] Ngah WSW, Fatinathan S, Yosop NA. Isotherm and kinetic studies on the adsorption of humic acid onto chitosan-H_2SO_4 beads. Desalination 2011;272:293–300.
[29] Rauf N, Tahir SS, Kang J-H, Chang Y-S. Equilibrium, thermodynamics and kinetics studies for the removal of alpha and beta endosulfan by adsorption onto bentonite clay. Chem Eng J 2012;192:369–76.
[30] Moussavi G, Talebi S, Farrokhi M, Sabouti RM. The investigation of mechanism, kinetic and isotherm of ammonia and humic acid co-adsorption onto natural zeolite. Chem Eng J 2011;171:1159–69.
[31] Koyuncu H, Kul AR. An investigation of Cu(II) adsorption by native and activated bentonite: kinetic, equilibrium and thermodynamic study. J Environ Chem Eng 2014;2:1722–30.
[32] Vadivelan V, Kumar KV. Equilibrium, kinetics, mechanism, and process design for the sorption of methylene blue onto rice husk. J Colloid Interface Sci 2005;286:90–100.
[33] Ahmad M, Lee S, Oh S-E, Mohan D, Moon D, Lee Y, Ok Y. Modeling adsorption kinetics of trichloroethylene onto biochars derived from soybean stover and peanut shell wastes. Environ Sci Pollut Res 2013;20:8364–73.
[34] Zou W, Han R, Chen Z, Jinghua Z, Shi J. Kinetic study of adsorption of Cu(II) and Pb(II) from aqueous solutions using manganese oxide coated zeolite in batch mode. Colloids Surf, A 2006;279:238–46.
[35] Foo KY, Hameed BH. Insights into the modeling of adsorption isotherm systems. Chem Eng J 2010;156:2–10.
[36] Limousin G, Gaudet JP, Charlet L, Szenknect S, Barthès V, Krimissa M. Sorption isotherms: a review on physical bases, modeling and measurement. Appl Geochem 2007;22:249–75.
[37] Vasanth Kumar K, Sivanesan S. Sorption isotherm for safranin onto rice husk: comparison of linear and non-linear methods. Dyes Pigm 2007;72:130–133.
[38] Febrianto J, Kosasih AN, Sunarso J, Ju Y-H, Indraswati N, Ismadji S. Equilibrium and kinetic studies in adsorption of heavy metals using biosorbent: a summary of recent studies. J Hazard Mater 2009;162:616–45.
[39] Potgieter JH, Potgieter-Vermaak SS, Kalibantonga PD. Heavy metals removal from solution by palygorskite clay. Miner Eng 2006;19:463–70.
[40] Hu J, Chen G, Lo IMC. Removal and recovery of Cr(VI) from wastewater by maghemite nanoparticles. Water Res 2005;39:4528–36.
[41] Babel S, Kurniawan TA. Cr(VI) removal from synthetic wastewater using coconut shell charcoal and commercial activated carbon modified with oxidizing agents and/or chitosan. Chemosphere 2004;54:951–67.
[42] Erdem M, Altundoğan HS, Tümen F. Removal of hexavalent chromium by using heat-activated bauxite. Miner Eng 2004;17:1045–52.
[43] Argun ME, Dursun S, Ozdemir C, Karatas M. Heavy metal adsorption by modified oak sawdust: thermodynamics and kinetics. J Hazard Mater 2007;141:77–85.
[44] Srivastava SK, Gupta VK, Mohan D. Removal of lead and chromium by activated slag - A blast-furnace waste. J Environ Eng 1997;123:461–8.
[45] Orhan Y, Buyukgungor H. The removal of heavy metals by using agricultural wastes. Water Sci Technol 1993;28:247–55.
[46] Chutia P, Kato S, Kojima T, Satokawa S. Arsenic adsorption from aqueous solution on synthetic zeolites. J Hazard Mater 2009;162:440–7.

[47] Ahalya N, Kanamadi RD, Ramachandra TV. Biosorption of chromium (VI) from aqueous solutions by the husk of Bengal gram (Cicer arientinum). Electron J Biotechnol 2005;8:258–64.
[48] Maji SK, Pal A, Pal T, Adak A. Adsorption thermodynamics of arsenic on laterite soil. J Surf Sci Technol 2007;23:161–76.
[49] Vijayaraghavan K, Padmesh TVN, Palanivelu K, Velan M. Biosorption of nickel(II) ions onto Sargassum wightii: application of two-parameter and three-parameter isotherm models. J Hazard Mater 2006;133:304–8.
[50] Demarchi CA, Debrassi A, Magro JD, Nedelko N, Ślawska-Waniewska A, Dłużewski P, Greneche J-M, Rodrigues CA. Adsorption of Cr(VI) on crosslinked chitosan–Fe(III) complex in fixed-bed systems. J Water Process Eng 2015;7:141–52.
[51] WHO. Guidelines for drinking-water quality: recommendations, volume 1. 3rd edition. World Health Organization; 2004.
[52] Onyango MS, Leswifi TY, Ochieng A, Kuchar D, Otieno FO, Matsuda H. Breakthrough analysis for water DE fluoridation using surface-tailored zeolite in a fixed bed column. Ind Eng Chem Res 2009;48:931–7.
[53] Podder MS, Majumder CB. Fixed-bed column study for As(III) and As(V) removal and recovery by bacterial cells immobilized on Sawdust/$MnFe_2O_4$ composite. Biochem Eng J 2016;105(Part A):114–35.
[54] Malkoc E, Nuhoglu Y, Dundar M. Adsorption of chromium(VI) on pomace—An olive oil industry waste: batch and column studies. J Hazard Mater 2006;138:142–51.
[55] Aksu Z, Gönen F. Biosorption of phenol by immobilized activated sludge in a continuous packed bed: prediction of breakthrough curves. Process Biochem 2004;39:599–613.
[56] Gupta VK, Gupta M, Sharma S. Process development for the removal of lead and chromium from aqueous solutions using red mud—an aluminium industry waste. Water Res 2001;35:1125–34.
[57] Yoon YH, Nelson JH. Application of gas adsorption kinetics I. A theoretical model for respirator cartridge service life. Am Ind Hyg Assoc J 1984;45:509–16.
[58] Thomas HC. Heterogeneous ion exchange in a flowing system. J Am Chem Soc 1944;66:1664–6.
[59] Foo KY, Lee LK, Hameed BH. Preparation of tamarind fruit seed activated carbon by microwave heating for the adsorptive treatment of landfill leachate: a laboratory column evaluation. Bioresour Technol 2013;133:599–605.
[60] Wang W-q, Li M-y, Zeng Q-x. Thermodynamics of Cr(VI) adsorption on strong alkaline anion exchange fiber. Trans Nonferr Met Soc China 2012;22:2831–9.
[61] Wang W, Li M, Zeng Q. Adsorption of chromium (VI) by strong alkaline anion exchange fiber in a fixed-bed column: experiments and models fitting and evaluating. Sep Purif Technol 2015;149:16–23.
[62] Agarwal GS, Bhuptawat HK, Chaudhari S. Biosorption of aqueous chromium(VI) by Tamarindus indica seeds. Bioresour Technol 2006;97:949–56.